

Bending Strength of Thin-Walled Centrifugal Concrete-Filled Steel Tubes

Ao-Yu Jiang, Ju Chen and Wei-Liang Jin

Department of Civil Engineering, Zhejiang University, China

Abstract: A study on the bending strength of design of thin-walled centrifugal concrete-filled steel tubes was conducted in this study. An accurate finite element model of centrifugal concrete-filled steel tubes was developed using the finite element program ABAQUS. Centrifugal concrete-filled steel tubes different cross sections and material properties were simulated in this study. The nonlinear finite element model was verified against the experimental results. Generally the finite element model could accurately simulate the bending strength of centrifugal concrete-filled steel tubes. Parametric study was conducted to investigate specimens having concrete tubes of different grades. Current AISC standard was used to predict the bending strength of thin-walled centrifugal concrete-filled steel tubes and empirical design equations are also proposed for simplicity. It is shown that the proposed method predicted the bending strength of thin-walled centrifugal concrete-filled steel tubes well.

Keywords: Bending strength, centrifugal concrete-filled steel tubes, design, finite element model

INTRODUCTION

Concrete-filled steel tubes are being increasingly used in architectural and structural application because of the excellent structural performance characteristics-high strength, high ductility, large stiffness and fire resistance. A significant amount of effort over the past 40 years has been aimed at developing a better understanding of circular concrete-filled steel tubes. The bending strength of circular concrete-filled steel has been studied by Lu and Kennedy (1994), Prion and Boehme (1994), Elchalakani *et al.* (2001), Nakamura *et al.* (2002), Han (2004) and Lu *et al.* (2008). In this study, the bending strength of thin-walled centrifugal concrete-filled steel tubes was investigated. The thin-walled centrifugal concrete-filled steel tubes were a thin-walled steel tube with a centrifugal concrete tube inside. Due to the effect of centrifugalization, the concrete tube inside the steel tube is relatively thin Jin *et al.* (2003), Chen *et al.* (2008) and Chen *et al.* (2009).

It can be quite costly and time consuming for experimental investigation, therefore, numerical method has been used in the area of in recent years. The finite element program (ABAQUS, 2004) has been widely used to investigate the behavior of concrete-filled steel tube. Han *et al.* (2006), Gupta *et al.* (2007), Ellobody *et al.* (2006) and Ellobody and Young (2006). Therefore, the finite element program ABAQUS is used to simulate the thin-walled centrifugal concrete-filled steel tubes in this study. The numerical investigation included specimens filled with different grades of concrete. The key issues of the finite element model such as material models for concrete and steel, concrete

cracking in the tension zone, composite action between the steel tube and its concrete core was considered.

The prediction of the bending strength of concrete-filled steel tubes has been studied by researchers to obtain a better prediction. Bergmann *et al.* (1995) and Han (2007) Current AISC (2005) also has the design provisions for the bending strength of concrete-filled steel tubes. However, those design methods are all for full concrete-filled steel tubes which are different from thin-walled centrifugal concrete-filled steel tubes. In this study, design equations for the bending strength of thin-walled centrifugal concrete-filled steel tubes were proposed and evaluated using finite element analysis results.

FINITE ELEMENT MODEL

General: The finite element program (ABAQUS, 2004) was used in the simulation. In order to accurately simulate the actual behavior of thin-walled centrifugal concrete-filled steel tubes, the main three components, namely the confined concrete, the circular steel tube and the interface between the concrete and the steel tube have to be modeled properly. In addition, careful attention was given to the choice of the element type and mesh size to combining a high level of numerical accuracy and stability with optimum computational efficiency. The load-displacement nonlinear analysis was performed in the analysis.

Finite element type and mesh: Different element types have been tried and solid elements were found to be more efficient in modeling the steel tube and the

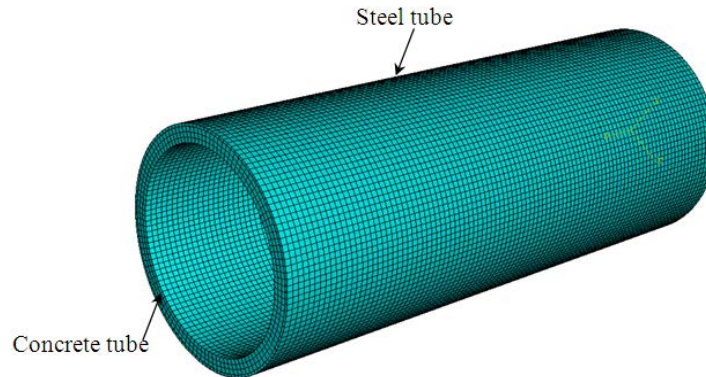


Fig. 1: Finite element mesh of specimen T4.5C25

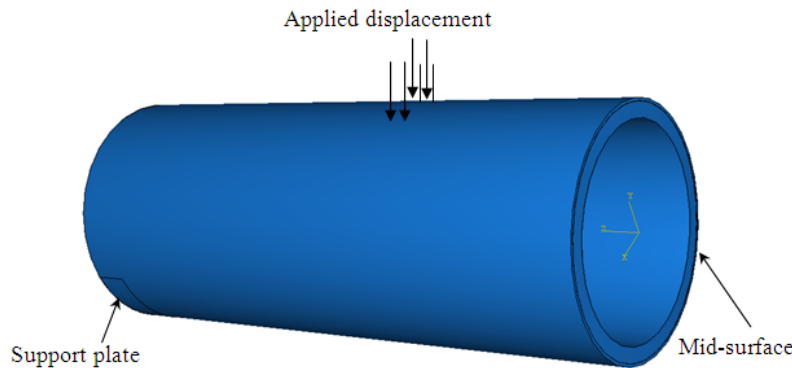


Fig. 2: Finite element model of thin-walled centrifugal concrete-filled steel tubes in bending

concrete tube as well as the clear defined boundaries of their elements. A first-order reduced integration 3D hexahedral solid element (C3D8R) and is chosen for concrete and steel tube. Different mesh sizes were tried in order to find a reasonable mesh that provides both accurate results and less computational time. It is found a mesh size of 1 (depth): 2 (width): 2 (length), for both steel and concrete elements, could achieve accurate results with optimum computational efficiency. Figure 1 shows the finite element mesh of a thin-walled concrete-filled steel tube of 4.5 mm plate thickness having an outer diameter of 200 mm with a concrete tube of 25 mm thickness (S4.5C25).

Boundary conditions and load application:

Following the test procedure, the beam was 4 points loaded. Only half of the beam was modeled for symmetry. In the finite element model, the support plate was modeled using rigid plate, whose motion is governed by the reference point. The reference point of the support plate was restrained against x and y directions displacement as well as y - and z -axes rotation but free to rotate about the x -axis. The loading was

applied by y direction displacement, as shown in Fig. 2. The load was applied in increments using the modified RIKS method available in the ABAQUS library. It uses the load magnitude as an additional unknown and solves simultaneously for loads and displacements. The Nonlinear Geometry Parameter (NLGEOM) was included to deal with the large displacement analysis.

MATERIALS MODELING

Steel tube: In the finite element model, the measured stress-strain curves of steel tubes were used. The experimental measured yield stresses (f_y) were 240, 300 and 360 MPa for steel tubes, respectively. The material behaviour provided by ABAQUS allows for a nonlinear stress-strain curve to be used. The first part of the nonlinear curve represents the elastic part up to the proportional limit stress with measured Young modulus (214,000, 212000 and 211,000 MPa for steel tubes with yield strengths of 240, 300 and 360 MPa, respectively) and Poisson's ratio equal to 0.30. Since the analysis involves large in-elastic strains, the nominal

Table 1: Geometry dimension and material properties of tested specimens

Specimen	D (mm)	t _s (mm)	t _c (mm)	L (mm)	f _s (MPa)	f _c (MPa)
S3.0C20	200	3.0	20.9	2000	364	44.5
S3.0C25	200	2.9	24.5	2000	300	57.5
S4.5C25	200	4.6	24.0	2000	240	57.5

(engineering) stress-strain curve was converted to a true stress and logarithmic plastic strain curve. The true stress and plastic true strain are specified in Abaqus (2004).

Concrete tube: Concrete constitutive model used is the concrete-damaged plasticity model in Abaqus (2004). Concrete is brittle material with different failure mechanisms in compression and tension, crushing in compression and cracking in tension. The concrete-damaged plasticity model adopts a unique yield function with no associated flow and a Drucker-Prager hyperbolic flow potential function to describe the plasticity of concrete. Therefore, independent uniaxial stress-strain relation for concrete both in compression and tension is the basic input data due to the difference in strength and failure mechanism in compression and tension.

Confined concrete model has used to simulate concrete-filled steel tube circular columns with a small value of the D/t ratio (Ellobody *et al.*, 2006). However, in this case, the concrete is not in triaxial compression state, therefore unconfined concrete model proposed by Hognestad *et al.* (1955) is used in this study. The concrete compressive stress-strain curve can be determined from Eq. (1) and (2) as below:

$$\sigma = f_c \left[\frac{2\varepsilon}{\varepsilon_0} - \left(\frac{\varepsilon}{\varepsilon_0} \right)^2 \right] \quad \text{for } 0 \leq \varepsilon \leq \varepsilon_0 \quad (1)$$

$$\sigma = f_c \left(1 - 0.15 \frac{\varepsilon - \varepsilon_0}{\varepsilon_u - \varepsilon_0} \right) \quad \text{for } \varepsilon_0 \leq \varepsilon \leq \varepsilon_u \quad (2)$$

where,

f_c = Concrete cube compressive strength

σ = The stress

ε = The strain

ε₀ = 0.002 is the strain corresponding to the maximum strength

ε_u = 0.0038 is the ultimate strain

The concrete cube compressive strength f_c is chosen from the material test results. The concrete tensile was assumed to be 10% of the concrete compression strength. The Poisson's ratio of concrete is taken as 0.2.

Concrete-steel tube interface: The interface model to simulate the interaction of steel and concrete in centrifugal concrete-filled steel tubes is the contact interaction in ABAQUS (2004). This method has been adopt by Lu *et al.* (2008) to simulate the interaction of

steel and concrete in full concrete-filled steel tubes under bending and was used in this study. This contact interaction model is capable of simulating the mechanical interactions of 2 deformable bodies at the interface. The surface-to-surface contact discretization is used, in which 2 of the contact surfaces are defined as master and slave surfaces, respectively. A small-sliding tracking approach is selected for the surfaces. The mechanical property of the contact interaction is defined along normal and tangential to the interface, respectively. The "hard contact" relation is selected as normal mechanical property. The tangential mechanical property of the contact interaction is simulated by an isotropic Coulomb friction model. The shear force between surfaces is calculated by friction coefficient and contact pressure. For centrifugal concrete-filled steel tubes, the coefficient of 0.25 obtained from full filled concrete steel tubes (Lu *et al.*, 2008) may be conservative. However, finite element analysis indicates this coefficient has small effect on the bending strengths of the specimens. Therefore, a friction coefficient of 0.25 is assigned in the calculation in this study.

VERIFICATION OF FINITE ELEMENT MODEL

The thin-walled centrifugal concrete-filled steel beams tested (Anonymous, 2003) were modeled in this study. The measured cross-section dimensions and material properties reported (Anonymous, 2003) were incorporated in the finite element model. The ultimate moments of the beams obtained from the Finite Element Analysis (M_{FEA}) are compared with the test results (M_{TEST}) in Table 1. The steel tubes were all manufactured from mild steel sheet having nominal plate thicknesses (t_s) of 3.0 and 4.5 mm. The thickness of the inside concrete tubes (t_c) were 20 and 25 mm. The specimen labeling system used in this study follows that specified in the experimental investigation study. The test specimens are labeled such that the thickness of steel tube and thickness of concrete tube could be identified from the label. The label S3.0C20 defines the specimen that has steel tube of 3.0 mm thickness (S3.0), concrete tube of 20 mm thickness (C20). The comparison indicates that the ultimate moments of beams predicted by the FEA are generally accurate. The mean value of M_{Test}/M_{FEA} is 0.98 with the maximum different of 5% (Table 2).

The moment versus mid-deflection of the specimen S3.0C20 obtained from tests and FEA are compared in Fig. 3. The comparison indicates that the FEA results

Table 2: Comparison of FEA results with test results

Specimen	Test	FEA	Comparison
	M_{TEST} (kN.m)	M_{FEA} (kN.m)	M_{TEST}/M_{FEA}
S3.0C20	53.4	56.2	0.95
S3.0C25	45.0	44.5	1.01
S4.5C25	60.0	61.5	0.98
		Mean	0.98

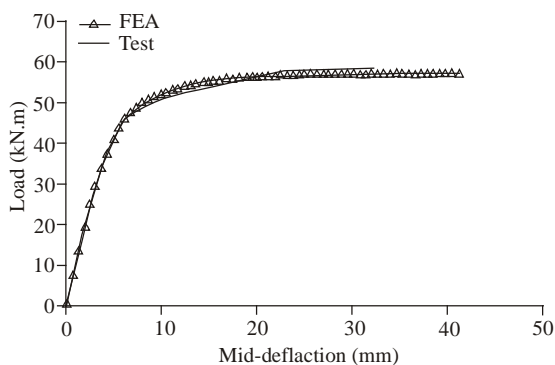


Fig. 3: Comparison of moment versus mid-deflection curves obtained from test and FEA

agree with the test results well. It could be found that the thin-walled centrifugal concrete-filled specimen has good ductility. In tests, severe vertical cracking was found at the tension side of concrete due to the tensile stress which was also found in the finite element model. When the load reach ultimate strength of specimens, bending failure occur in the mid of the specimen. The comparison indicates that the FEA could simulate the behavior of thin-walled centrifugal concrete-filled specimen with reasonable accuracy.

PARAMETRIC STUDY

The verification showed that the finite element model of thin-walled centrifugal concrete-filled steel

tubes in bending was reasonably accurate. Hence, parametric study was carried out to investigate the bending strengths of thin-walled centrifugal concrete-filled steel tubes having different cross sections and material properties. The cross-section dimensions are shown in Table 3 using the symbols defined in Fig. 4. The specimens were divided into 3 series with different thickness and yield strength of steel tubes. Each series of specimens has 6 specimens. The 6 specimens investigated in each group had concrete cube strengths of 30, 40, 50, 60, 70 and 80 MPa, respectively. The measured stress-strain curves of steel tubes investigated in the bending tests (Anonymous, 2003) were used in finite element analysis of Series 1, 2 and 3, respectively.

AISC STANDARD DESIGN METHOD

General: The current (AISC, 2005) has the provisions for flexural strength of concrete-encased and filled members. The design strength shall be determined using one of the following methods:

- Based on the first yield in the tension flange of the composite section.
- Based on the plastic flexural strength of the steel section alone.
- Based on the plastic flexural strength of the composite section or the strain-compatibility method.

Method (c) is applicable only when shear connectors are provided along the steel section and reinforcement of the concrete encasement meets the specified detailing requirements. In this study, the design strengths for thin-walled centrifugal concrete-filled tubes are calculated using the 3 methods above. Although there is no shear connects used in the

Table 3: Geometry dimension and material properties of specimens in parametric study

Specimen	D (mm)	t_s (mm)	t_c (mm)	L (mm)	f_s (MPa)	f_c (MPa)
S3.0C20A	200	3.0	20.0	2000	364	30
S3.0C20B	200	3.0	20.0	2000	364	40
S3.0C20C	200	3.0	20.0	2000	364	50
S3.0C20D	200	3.0	20.0	2000	364	60
S3.0C20E	200	3.0	20.0	2000	364	70
S3.0C20F	200	3.0	20.0	2000	364	80
S3.0C25A	200	3.0	25.0	2000	300	30
S3.0C25B	200	3.0	25.0	2000	300	40
S3.0C25C	200	3.0	25.0	2000	300	50
S3.0C25D	200	3.0	25.0	2000	300	60
S3.0C25E	200	3.0	25.0	2000	300	70
S3.0C25F	200	3.0	25.0	2000	300	80
S4.5C25A	200	4.5	25.0	2000	240	30
S4.5C25B	200	4.5	25.0	2000	240	40
S4.5C25C	200	4.5	25.0	2000	240	50
S4.5C25D	200	4.5	25.0	2000	240	60
S4.5C25E	200	4.5	25.0	2000	240	70
S4.5C25F	200	4.5	25.0	2000	240	80

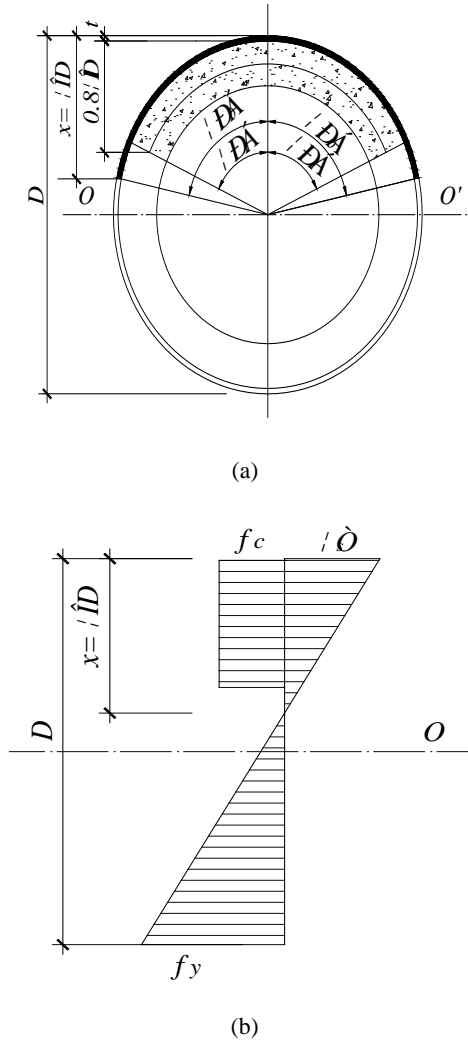


Fig. 6: Equivalent compressive stress zone of concrete tube in thin-walled centrifugal concrete filled steel tube section

$$Z_1 = 2 \int_0^{\pi\alpha_0} \sigma_x dA_s = \frac{A_s \sigma_s}{2\pi\xi} [(2\xi - 1)\pi\alpha_0 + \sin \pi\alpha_0] \quad (8)$$

$$\left(dA_s = \frac{A_s}{2\pi} d\theta \right)$$

$$M_{z1} = 2 \int_0^{\pi\alpha_0} \sigma_x \frac{D}{2} \cos \theta dA_s = \frac{A_s \sigma_s}{4\pi\xi} [(2\xi - 1) \sin \pi\alpha_0 + \frac{\pi\alpha_0}{2} + \frac{\sin 2\pi\alpha_0}{4}] \quad (9)$$

The force (T_1) and moment (M_{T1}) of compression zone of steel tube could be calculated using Eq. (10) and (11), respectively:

$$T_1 = 2 \int_{\pi\alpha_0}^{\pi} \sigma_x dA_s = \frac{A_s f_y}{2\pi(1-\xi)} [(2\xi - 1)(\pi - \pi\alpha_0) - \sin \pi\alpha_0] \quad (10)$$

$$M_{T1} = 2 \int_{\pi\alpha_0}^{\pi} \sigma_x y dA = \frac{A_s f_y D}{4\pi(1-\xi)} [-(2\xi - 1) \sin \pi\alpha_0 + \frac{\pi}{2} (1 - \alpha_0) - \frac{\sin 2\pi\alpha_0}{4}] \quad (11)$$

Force (Z_c) and moment (M_{zc}) of the concrete tube:

The force (T_1) and moment (M_{T1}) of compression zone of steel tube could be calculated using Eq. (12) and (13), respectively:

$$Z_c = \alpha_1 A_c f_c^0 \quad (12)$$

$$M_{zc} = 2 \int_0^{\pi\alpha_1} f_c^0 y dA_c = A_c f_c^0 D_c \frac{\sin \pi\alpha_1}{2\pi} \quad (13)$$

Equilibrium equations: The equilibrium equations of force and moment of the specimen sections could be written as Eq. (14) and (15):

$$0 = Z_c + Z_1 + T_1 \quad (14)$$

$$M = M_{zc} + M_{z1} + M_{T1} \quad (15)$$

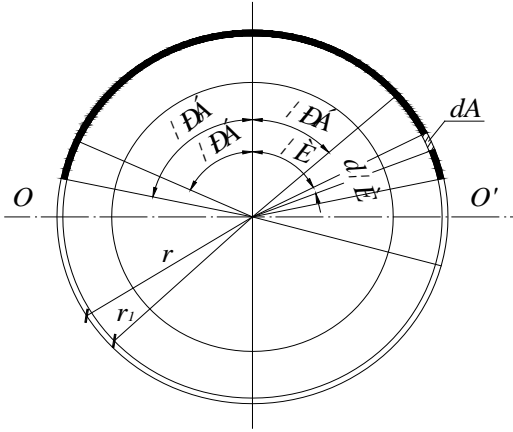
Proposed equations for the third method: The main difference between the first and 3rd methods is that the steel tube has the plastic deformation. The stress distribution of the composite section using the third method is shown in Fig. 7 based on which the design equations are developed.

Steel tube: It is assumed that the height of compression zone of steel tube is, $\xi = \frac{x}{D}$ and the corresponding angle is $\pi\alpha_0$. The relationship between ξ and $\pi\alpha_0$ could be obtained from Fig. 5 as Eq. (3) and (4).

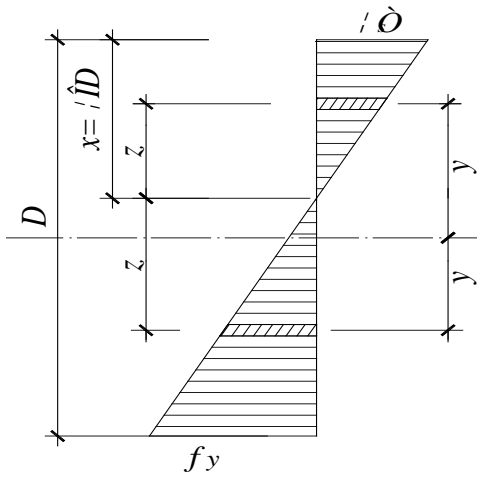
The height of compression zone of steel tube with the stress less than f_y (elastic part) is assumed as (βx) and β could be calculated using Eq. (16), the height plastic part $(1-\beta x)$ could be calculated using Eq. (17):

$$\beta = \frac{\varepsilon_0}{\varepsilon_u} = \frac{f_y}{0.003 E_s} \quad (16)$$

$$(1 - \beta)x = r - r_c \cos \alpha_1 \quad (17)$$



(a)



(b)

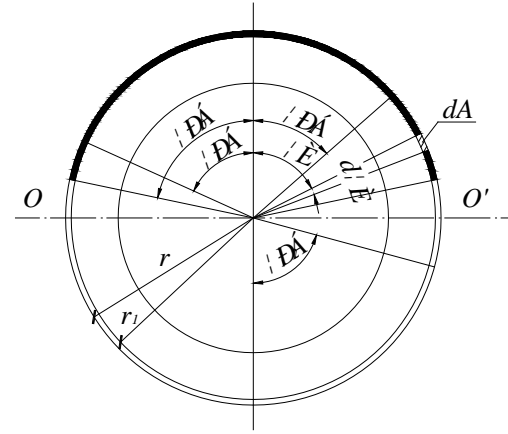
Fig. 7: Stress distribution in thin-walled centrifugal concrete-filled steel tube section according to the first method specified in AISC standard

The height of elastic part of tension zone of steel tube is also (βx) and could be expressed as Eq. (18) and could be rewritten as Eq. (19). Thus the angle correspond to the plastic part of tension zone of steel tube (α_2) could be calculated using Eq. (20):

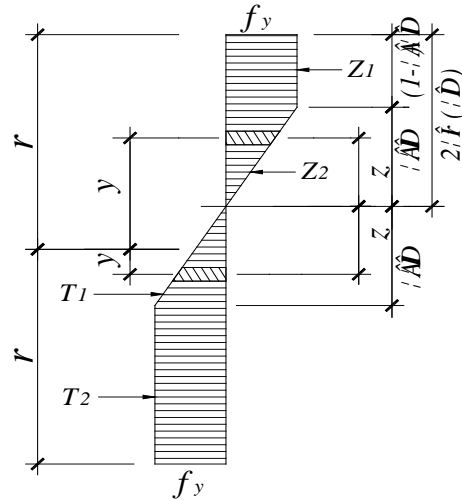
$$\beta x = (r - r_c \cos \alpha_2') - x \quad (18)$$

$$\cos \alpha_2' = 1 - 2(1 + \beta)\xi \quad (19)$$

$$\alpha_2 = 1 - \alpha_2' \quad (20)$$



(a)



(b)

Fig. 8: Stress distribution in thin-walled centrifugal concrete-filled steel tube section according to the first method specified in AISC standard

Concrete tube: The height of equivalent rectangular stress block of concrete compression zone is x_0 with corresponding angle of $\pi\alpha$ and could be determined as Eq. (21) and (22), respectively:

$$x_0 = 0.8\xi D = r - r_c \cos \pi\alpha \quad (21)$$

$$\cos \pi\alpha = (1 - 1.6\xi) \frac{r}{r_c} \quad (22)$$

Force and moment: The force (Z_1) and moment (M_{Z1}) of the plastic part (Rectangular zone) of compression zone could be determined as Eq. (23) and (24), respectively, according to Fig. 8.

$$Z_1 = \alpha_1 A_s f_y \quad (23)$$

$$M_{z1} = 2 \int_0^{\pi\alpha_1} f_y y dA \quad (dA = \frac{A_s}{2\pi} d\theta) \quad (24)$$

And y is approximate taken as $y = r \cos\theta$, so that Eq. (24) could be rewritten as Eq. (25).

$$M_{z1} = \frac{A_s f_y r}{\pi} \int_0^{\pi\alpha_1} \cos\theta d\theta = \frac{A_s f_y r}{\pi} \sin\pi\alpha_1 \quad (25)$$

The force (Z_2) and moment (M_{Z2}) of the elastic part (Triangle zone) of compression zone could be calculated using Eq. (26) and (27), respectively:

$$\begin{aligned} Z_2 &= 2 \int_{\pi\alpha_1}^{\pi\alpha_0} \sigma_x dA \\ &= \frac{A_s f_y}{2\pi\beta\xi} \int_{\pi\alpha_1}^{\pi\alpha_0} (2\xi - 1 + \cos\theta) d\theta = A_s f_y k_z \quad (26) \end{aligned}$$

where,

$$\begin{aligned} k_z &= \frac{1}{2\beta\xi} [(2\xi - 1)(\alpha_0 - \alpha_1) + \frac{\sin\pi\alpha_0 - \sin\pi\alpha_1}{\pi}] \\ M_{z2} &= 2 \int_{\pi\alpha_1}^{\pi\alpha_0} \sigma_x y dA \\ &= \frac{A_s f_y r}{2\pi\beta\xi} \int_{\pi\alpha_1}^{\pi\alpha_0} (2\xi - 1 + \cos\theta) \cos\theta d\theta \\ &= A_s f_y r \frac{m_z}{\pi} \quad (27) \end{aligned}$$

where,

$$\begin{aligned} m_z &= \frac{1}{2\beta\xi} [(2\xi - 1)(\sin\pi\alpha_0 - \sin\pi\alpha_1) \\ &+ \frac{\pi}{2} (\alpha_0 - \alpha_1) + \frac{\sin 2\pi\alpha_0 - \sin 2\pi\alpha_1}{4}] \end{aligned}$$

The tensile stress in the steel tube away from the neutral axis z mm could be calculated using Eq. (28). The force (T_1) and moment (M_{T1}) of the elastic part (Triangle zone) of tension zone could be calculated using Eq. (29) and (30), respectively:

$$\sigma_x = \frac{f_y}{2\beta\xi} (2\xi - 1 + \cos\theta) \quad (28)$$

$$T_1 = 2 \int_{\pi\alpha_0}^{\pi\alpha_2'} \sigma_x dA = A_s f_y k_t \quad (29)$$

where,

$$k_t = \frac{1}{2\beta\xi} [(2\xi - 1)(\alpha_2' - \alpha_0) + \frac{\sin\pi\alpha_2' - \sin\pi\alpha_0}{\pi}]$$

$$M_{T1} = 2 \int_{\pi\alpha_0}^{\pi\alpha_2'} \sigma_x y dA = A_s f_y r \frac{m_t}{\pi} \quad (30)$$

where,

$$\begin{aligned} m_t &= \frac{1}{2\beta\xi} [(2\xi - 1)(\sin\pi\alpha_2' - \sin\pi\alpha_0) \\ &+ \frac{\pi}{2} (\alpha_2' - \alpha_0) + \frac{\sin 2\pi\alpha_2' - \sin 2\pi\alpha_0}{4}] \end{aligned}$$

The force (T_2) and moment (M_{T2}) of the plastic part (Rectangular zone) of tension zone could be calculated using Eq. (31) and (32), respectively:

$$T_2 = -\alpha_2 A_s f_y \quad (31)$$

$$M_{T2} = 2 \int_{\pi\alpha_2'}^{\pi} -f_y y dA = \frac{-A_s f_y r}{\pi} \int_{\pi\alpha_2'}^{\pi} \cos\theta d\theta = \frac{A_s f_y r}{\pi} \sin\pi\alpha_2 \quad (32)$$

Since the tensile strength of concrete is neglected, only the compressive strength is considered. The force (Z_C) and moment (M_{ZC}) could be calculated as Eq. (33) and (34), respectively:

$$Z_C = \alpha A_c f_c^0 \quad (33)$$

$$M_{ZC} = 2 \int_0^{\pi\alpha} f_c^0 y dA = A_c f_c^0 r_c \frac{\sin\pi\alpha}{\pi} \quad (34)$$

Equilibrium equations: The force and moment should be balanced and the equilibrium equations could be written as below:

$$0 = Z_c + Z_1 + Z_2 + T_1 + T_2 \quad (35)$$

$$M = M_{ZC} + M_{Z1} + M_{Z2} + M_{T1} + M_{T2} \quad (36)$$

Table 4: Comparison of FEA results with AISC design predictions

Specimen	FEA	Design			Comparison		
	M_{FEA} (kN.m)	$M_{Design-1}$ (kN.m)	$M_{Design-2}$ (kN.m)	$M_{Design-3}$ (kN.m)	$M_{FEA}/M_{Design-1}$	$M_{FEA}/M_{Design-2}$	$M_{FEA}/M_{Design-3}$
S3.0C20A	49.1	36.2	43.0	48.2	1.36	1.14	1.02
S3.0C20B	52.3	37.2	43.0	49.9	1.41	1.22	1.05
S3.0C20C	54.6	38.0	43.0	51.3	1.44	1.27	1.06
S3.0C20D	57.3	38.9	43.0	52.5	1.47	1.33	1.09
S3.0C20E	59.2	39.7	43.0	53.5	1.49	1.38	1.11
S3.0C20F	60.8	40.5	43.0	54.4	1.50	1.41	1.12
S3.0C25A	47.6	30.7	35.5	41.7	1.55	1.34	1.14
S3.0C25B	49.5	31.7	35.5	43.1	1.56	1.39	1.15
S3.0C25C	50.8	32.5	35.5	44.1	1.56	1.43	1.15
S3.0C25D	52.2	33.3	35.5	45.0	1.57	1.47	1.16
S3.0C25E	53.6	34.0	35.5	45.7	1.58	1.51	1.17
S3.0C25F	54.3	34.6	35.5	46.2	1.57	1.53	1.18
S4.5C25A	55.0	35.9	42.2	48.8	1.53	1.30	1.13
S4.5C25B	57.7	36.7	42.2	50.3	1.57	1.37	1.15
S4.5C25C	59.2	37.7	42.2	51.6	1.57	1.40	1.15
S4.5C25D	60.9	38.6	42.2	52.6	1.58	1.44	1.16
S4.5C25E	62.6	39.3	42.2	53.4	1.59	1.48	1.17
S4.5C25F	63.4	40.0	42.2	54.1	1.59	1.50	1.17
				Mean	1.53	1.38	1.13
				COV	0.045	0.076	0.041

Substituting the equations of force and moment above, Eq. (35) and (36) could be rewritten as Eq. (37) and (38), respectively:

$$0 = \alpha A_c f_c^0 + A_s f_s (\alpha_1 + k_z) - A_s f_s (\alpha_2 - k_t) \quad (37)$$

$$M = A_c f_c^0 r_c \frac{\sin \pi \alpha}{\pi} + \frac{A_s f_s r}{\pi} \left[(\sin \pi \alpha_1 + m_z) + (\sin \pi \alpha_2 + m_t) \right] \quad (38)$$

Solution and comparison: It is difficult to get the analytic solutions of the Eq. (14), (15), (37) and (38), there the trial and error method is used to get the results. The value of x is firstly assumed and substituted into the force equilibrium equation. The value of x which could balance the force is determined by try and error. Then the determined x is substituted into the moment equilibrium equation to get the value of bending strength (M).

The design strengths predicted according to AISC standard were compared with FEA results in Table 4. It is shown that the design strengths predicted by method 1 and 2 are very conservative and could be considered as lower boundary. The mean value of $M_{FEA}/M_{Design-1}$ and $M_{FEA}/M_{Design-2}$ is 1.53 and 1.38, with the corresponding Coefficient of Variation (COV) of 0.045 and 0.076 respectively. The design strengths predicted by method 3 generally agree with the FEA results well. The value of $M_{FEA}/M_{Design-3}$ is 1.13 and the corresponding coefficient of variation is 0.041. The comparison indicates that even there is no shear

connection between the steel tube and concrete tube, method 3 specified in AISC standard could conservatively predict the bending strength of thin-walled centrifugal concrete-filled steel tubes with reasonable accuracy. The reason may be that the load carried by the concrete tube is relatively small due to the thin thickness of the concrete tube so that the cohesion between the concrete tube and steel tube is sufficient.

PROPOSED METHODOLOGY

The design methods above are complex and not easy to use. Therefore, an empirical method by simply adding the strengths of steel tube and concrete tube together is proposed by in this study. Since the area of concrete tube is much smaller compared with that full concrete-filled steel tube, it may consider that concrete tube has some enhancement effect on the bending strength of steel tube. Therefore, empirical coefficient is used to taken into consideration the enhancement of concrete tube to the steel tube. The design equation is written as Eq. (39). The design strengths predicted by the proposed equation are compared with FEA results in Table 5. The mean value of $M_{FEA}/M_{Proposed}$ is 1.00 with the corresponding coefficient of variation of 0.026. The maximum difference between the predictions and FEA results is 5%. The comparison indicates that the proposed equation predicts the bending strength of thin-walled centrifugal concrete-filled steel tubes accurately:

$$M = (0.0137\psi^2 - 0.19\psi + 1.69) \times M_s \quad (39)$$

Table 5: Comparison of FEA results with predictions obtained from proposed method

Specimen	FEA	Design	Comparison
	M_{FEA} (kN.m)	$M_{Proposed}$ (kN.m)	$M_{FEA}/M_{Proposed}$
S3.0C20A	49.1	50.1	0.98
S3.0C20B	52.3	54.1	0.97
S3.0C20C	54.6	57.1	0.96
S3.0C20D	57.3	59.3	0.97
S3.0C20E	59.2	61.0	0.97
S3.0C20F	60.8	62.3	0.98
S3.0C25A	47.6	45.9	1.04
S3.0C25B	49.5	48.8	1.01
S3.0C25C	50.8	50.8	1.00
S3.0C25D	52.2	52.2	1.00
S3.0C25E	53.6	53.2	1.01
S3.0C25F	54.3	54.0	1.01
S4.5C25A	55.0	52.2	1.05
S4.5C25B	57.7	56.0	1.03
S4.5C25C	59.2	58.6	1.01
S4.5C25D	60.9	60.5	1.01
S4.5C25E	62.6	61.9	1.01
S4.5C25F	63.4	63.0	1.01
		Mean	1.00
		COV	0.026

where,

M_s : The plastic bending strength of the steel section

ψ : Defined as $\psi = A_s f_y / A_c f_c$

A_s : The cross section area of steel tube

f_y : The yield strength of steel

A_c : The cross section area of steel tube

f_c : The concrete compressive strength

CONCLUSION

This study focus on the bending strength of thin-walled centrifugal concrete-filled steel tubes. An accurate finite element model was developed and verified against experimental results. It is shown that the finite element model was able to simulate the studied beams accurately. Therefore, a parametric study was conducted using the verified finite element model. Four series of thin-walled centrifugal concrete-filled steel tubes having different cross-section dimensions and material properties were investigated. It is shown that the steel strength has significant effect on the bending capacity of thin-walled centrifugal concrete-filled steel tubes. Based on the numerical investigation, the design method specified in current AISC standard was evaluated in this study. It is shown that the design strengths predicted by method 1 and 2 are very conservative and could be considered as lower boundary. The design strengths predicted by method 3 generally agree with the FEA results well. Since the design method 1 and 3 are difficult to be calculated, empirical equations for bending strength of thin-walled centrifugal concrete-filled steel tubes was proposed for simplicity. It is shown that the proposed method predict the specimen strengths with reasonable accuracy.

ACKNOWLEDGMENT

The research study described in this paper was supported by grant from National Key Technology R&D Program (2011BAJ09B03), National Natural Science Foundation of China (51108409), research projects from Science and Technology Department of Zhejiang Province (2011C23102) and (2011R10064).

NOMENCLATURE

- A_c = Cross section area of concrete tubes
- A_s = Cross section area of steel tubes
- D = Outer diameter of cross section of specimen
- E_s = Elastic modulus of steel tube
- f_c = Compressive strength of concrete
- f_y = Yield strength of steel
- L = Length of specimen
- M = Bending strength
- $M_{Design-1}$ = Strength predicted using method 1 specified in AISC standard
- $M_{Design-2}$ = Strength predicted using method 2 specified in AISC standard
- $M_{Design-3}$ = Strength predicted using method 3 specified in AISC standard
- M_{FEA} = Strength obtained from FEA
- $M_{Proposed}$ = Strength predicted using proposed method
- M_s = Bending strength of steel tube section
- M_{TEST} = Strength obtained from test results
- r = Outer radius of cross section of specimen
- r_c = Average radius of concrete tube
- r_1 = Outer radius of concrete tube
- r_2 = Inner radius of concrete tube
- t_c = Thickness of concrete tube
- t_s = Thickness of steel tube
- σ = Stress
- ε = Strain
- ε_0 = The strain corresponding to the maximum concrete strength
- ε_u = The ultimate strain of concrete

REFERENCES

- ABAQUS, 2004. Analysis User's Manual. Version 6.5, ABAQUS, Inc.
- ACI, Committee 318 (ACI 318), 2005. Building Code Requirements for Structural Concrete and Commentary. American Concrete Institute, Detroit, USA.
- AISC, 2005. Specification for Structural Steel Buildings. American Institution of Steel Construction (AISC), ANSI/AISC 360-05, Chicago, Illinois.

- Anonymous, 2003. Bending tests of thin-walled centrifugal concrete-filled steel tubes. Technical Report, Zhejiang Electric Power Design Institute, (In Chinese).
- Bergmann, R., C. Matsui, C. Meinsma and D. Dutta, 1995. Design Guide for Concrete-Filled Hollow Section Columns under Static and Seismic Loading. Verlag TUV, Rheinland.
- Chen, J., W.L. Jin and J. Fu, 2008. Experimental investigation of thin walled centrifugal concrete-filled steel tubes under torsion. *Thin. wall. Struct.*, 46(10): 1087-1093.
- Chen, J., J. Chen and W.L. Jin, 2009. Design of thin-walled centrifugal concrete-filled steel tubes under torsion. *Thin. wall. Struct.*, 47(3): 271-276.
- Elchalakani, M., X.L. Zhao and R.H. Grzebieta, 2001. Concrete-filled circular steel tubes subjected to pure bending. *J. Constr. Steel. Res.*, 57(11): 1141-68.
- Ellobody, E. and B. Young, 2006. Design and behaviour of concrete-filled cold-formed stainless steel tube columns. *Eng. Struct.*, 28 (5): 716-728.
- Ellobody, E., B. Young and D. Lamc, 2006. Behavior of normal and high strength concrete-filled compact steel tube circular stub columns. *J. Constr. Steel. Res.*, 62(8): 706-715.
- Gupta, P.K., S.M. Sarda and M.S. Kumar, 2007. Experimental and computational study of concrete filled steel tubular columns under axial loads. *J. Constr. Steel. Res.*, 63(1): 182-193.
- Han, L.H., 2004. Flexural behaviour of concrete-filled steel tubes. *J. Constr. Steel. Res.*, 60(2): 313-337.
- Han, L.H., H. Lu, G.H. Yao and F.Y. Liao, 2006. Further study on the flexural behaviour of concrete-filled steel tubes. *J. Constr. Steel. Res.*, 62(6): 554-565.
- Han, L.H., 2007. Concrete-Filled Steel Tube Structures-Theory and Design. 2nd Edn., Science Press, Beijing.
- Hognestad, E., N.W. Hanson and D. McHenry, 1955. Concrete stress distribution in ultimate strength design. *ACI. J.*, 52(4): 455-479.
- Jin, W.L., C. Qu and Y. Yu, 2003. Experimental study on centrifugal concrete-filled steel tubes under bending and torsion. *J. Zhejiang Univ, Sci.*, 4(5): 565-572.
- Lu, Y.Q. and D. Kennedy, 1994. Flexural behaviour of concrete-filled hollow structural sections. *Can. J. Civil Eng.*, 21: 111-130.
- Lu, H., L.H. Han and X.L. Zhao, 2009. Analytical behavior of circular concrete-filled thin-walled steel tubes subjected to bending. *Thin. wall. Struct.*, 47(3): 346-358.
- Nakamura, S., Y. Momiyana, T. Hosaka and K. Homma, 2002. New technologies of steel/concrete composite bridge. *J. Constr. Steel. Res.*, 58(1): 99-130.
- Prion, H.G.L. and J. Boehme, 1994. Beam-column behaviour of steel tubes filled with high strength concrete. *Can. J. Civil Eng.*, 21: 207-218.